

Complex study of e-glass corrosion

Both the static and dynamic corrosion tests of E-glass were used for different conditions — temperature, glass surface to solution volume ratio (S/V), solution flow rate (F) and F/S ratio. Results obtained for glass fibres were compared with the ones for glass grains and planar samples. Evaluation of experimental results by kinetic model shows that the change of glass surface should be taken into account in the case of fibres corrosion. The total incongruent process of dissolution could be explained as congruent dissolution of glass accompanied by back precipitation of SiO₂ or silicates. In most cases, more than 90 % of SiO₂ precipitates back. The second possible explanation, i.e. SiO₂ network dissolution accompanied by selective leaching of Ca, B and Al, is not very probable. The glass sample shape can influence the estimation of dissolution rate. Up to now, with existing kinetic models, the dissolution rates evaluated from experiments with different shapes of glass (fibres, grains, planar) cannot be used as materials properties.

INTRODUCTION

The glass corrosion process was described using many model approaches in the last decades [1]. The kinetic model based on mass balance of dissolving glass components in glass-corrosion solution system was suggested in our previous works [2-4]. In this model, the time dependence of normalized leach amount of glass components *i* can be described using simple equation :

$$NL_i = \frac{B}{K} [1 - \exp(-Kt)] + Wt \quad (1)$$

The Eq. 1 is based on the mass balance of component *i* in solution :

$$\frac{dc_i}{dt} = \frac{S}{V} \left(1 - k^-\right) \frac{k^+ D/h}{k^+ + D/h} (c_s - c_i) - \frac{F}{V} c_i \quad (2)$$

As it was shown in [4], for the simpler cases, the values of B, K and W

Des tests de corrosion dynamiques et statiques du verre E ont été réalisés sous différentes conditions, température, rapport surface volume (S/V), débit (F) et facteur F/S. Les résultats obtenus sur des fibres de verre sont comparés à ceux mesurés sur du verre plan et du verre broyé en grains. L'évaluation des résultats expérimentaux au moyen de modèle cinétique montre que les changements à la surface du verre devraient être pris en compte dans le cas de la corrosion des fibres. Le procédé pourrait être expliqué comme une dissolution du verre accompagné de précipitations de SiO₂ ou de silicates. Dans la plupart des cas, plus de 90 % de SiO₂ précipite. La seconde explication possible, c'est-à-dire le fait que la dissolution du réseau de SiO₂ est accompagnée d'une lixiviation sélective du Ca, du B et de l'Al, est peu probable. La forme de l'échantillon de verre influence les estimations du taux de dissolution. Avec les modèles cinétiques existants, les taux de dissolution évalués expérimentalement sur des échantillons de différentes formes (fibre, grains, plan) ne peuvent plus être utilisés automatiquement comme une propriété des matériaux.

Glass composition [wt. %]

sample	SiO ₂	CaO	Al ₂ O ₃	B ₂ O ₃	K ₂ O	MgO	TiO ₂	NaO ₂	F	Fe ₂ O ₃	Cr ₂ O ₃	total
fibres	54.2	22.9	13.8	6.4	0.48	0.41	0.33	0.30	0.32	0.29	-	99.43
grains	53.8	22.8	14.2	6.9	0.48	0.52	0.37	0.39	0.24	0.13	0.008	99.84
planar	54.3	22.7	13.9	6.6	0.51	0.50	0.35	0.32	0.51	0.15	0.007	99.99

Density and specific surface

sample	density ρ [g/cm ³]	specific surface Sg [m ² /g]
VL	2.5417 \pm 0.0034	0.1174 \pm 0.0008
DR	2.6215 \pm 0.0030	0.0163 \pm 0.0015

Table 1. Chemical composition of fibers, grains and planar samples in wt. %

Table 2. Density and specific surface of fibrous samples and grains

can be estimated as functions of test conditions as F, V, S and of parameters characterising the partial corrosion processes (rate constant of surface reaction k^+ , thickness of precipitated layer h , diffusion coefficient of surface reaction products in precipitated layer D , saturated concentration of component i in solution c_s and k , characterising back precipitation, i.e. the ratio between back precipitated and dissolved component i . The Eq. 1 is often used as empirical equation, describing the time dependencies of NL^i satisfactorily – e.g. in [5] it was used for successful description of corrosion of E-glass used as insulation in nuclear power plants reactors.

The aim of our study is to compare the initial and final dissolution rates obtained under different test conditions (S/V, F, F/S, static or dynamic conditions) and for different glass samples (fibres, grains, planar samples) using the existing kinetic dissolution model. We would also like to demonstrate, that the dissolution rates obtained by empirical use of the model, although useful for description of particular glass dissolution process, cannot be automatically used as real material properties. As E-glass was available in all different shapes, i.e. as fibres, grains and as planar samples, it was chosen as materials tested.

EXPERIMENTAL PART**GLASS SAMPLES**

Corrosion tests were made on three different shapes prepared from of E-glass (Eutal type) sam-

ples. The chemical composition was obtained using X-ray fluorescence analysis (XFA) and it is given in table 1.

The fibres for corrosion testing were drawn using industrial Pt furnace but without lubrication. Every strand of fibres consisted of approx. 800 elementary fibres. The material for grains was obtained also from industrial process during the exchange of Pt furnaces. The glass remained in furnace was annealed for 8 hours at 550 °C and then the grains were prepared in centrifugal mill (Retsch). For experiments, the fraction 0.315-0.5 mm was used, obtained according to DIN 4188. The samples were cleared from Fe particles, washed in acetone and in ultrasonic bath. The planar samples were prepared by melting of E-glass cullet in Pt/Rh crucible at 1450 °C for 1.5 hours. For better homogeneity, the melt was 3x stirred during the melting. The glass was annealed at 550 °C for 4 hours. Polished planar samples (approx. 1x1x0.1 [cm]) were used for testing. The exact dimensions of each sample were obtained using optical microscopy and image analysis LUCIA. The density of grains and fibres were obtained by pycnometric method using liquid He, the specific surface was measured using BET method with Kr gas. The results are summarised in table 2.

The initial mean value of fibres thickness 12.7 \pm 0.2 Gm was evaluated by optical microscopy and image analysis sample of 300 fibres. Particle size distribution in

crushed sample was determined with laser diffractometry. The initial mean value of particle's size was 509.4 Gm and the shape factor 3.6 was calculated according to DIN 66144.

CORROSION SOLUTIONS

Two corrosion solutions were used: 2M HCl and 0.2M NaOH prepared using deionised water.

CORROSION TESTS

Static and single-pass flow-through (SPFT) tests were used for obtaining glass dissolution rates. For static tests, the samples were given into polyethylene bottles with corrosion solution. In the case of planar samples, the contact with bottle was avoided. The bottles were placed into the stirred water bath (JULABO SW 21C), stirring frequency was 0.75 s⁻¹. Time of exposition was between 1 and 32 days. The tests were done for three different S/V ratios: 12, 117 and 1174 m⁻¹. The details of SPFT tests were described e.g. in [6]. During this test, the flow of corrosion solution was maintained using peristaltic pump (PCD 83.4 K Kou.il s.r.o.). The samples were in polyethylene cells with polyethylene frits (3 Gm pores). The cells were placed in water bath (JULABO SW 21C). Time of exposition for SPFT tests was between 1 and 4 days. The different solution flow rates (58-250 ml.d⁻¹) and F/S (0.027-0.308 Gm.s⁻¹) ratios were used in the study. After corrosion test, the solution was filtered when necessary (FILTRAK 389) and analysed for Al,

Si, B and Ca using AAS or ICP/OES or spectrophotometry.

RESULTS AND DISCUSSION

In case of fibrous and powder glass samples that are subject to significant mass loss (typically more than 10 %) during the test, the S/V ratio used to calculate the normalized mass loss must be corrected over time. This correction is implemented by means of a shrinking core model [7] in which the fibres and the powder grains are considered as cylinders and spheres respectively. In the case of planar samples, the changes of S were very small and could be neglected. The altered glass mass percentage (AG %) is defined by:

$$AG\% = 100 \times \frac{c_B V}{m_0 x_B} \quad (4)$$

where c_B is boron (alteration tracer element) concentration, V is volume of the corrosion solution, m_0 is initial sample mass, and x_B is boron mass fraction in the glass.

The geometric surface area S_i of the fibrous sample at the time interval i is

$$S_{cylinder,i} = \frac{n\pi d_0^2}{2} \left(\frac{100 - (AG\%)}{100} \right)^{\frac{1}{2}} + n\pi d_0 l \left(\frac{100 - (AG\%)}{100} \right)^{\frac{1}{2}} \quad (5)$$

The geometric surface area S_i of the powder glass at the time interval i is

$$S_{sphere,i} = \frac{6m_0}{d_0 \rho} \left(\frac{100 - (AG\%)}{100} \right)^{\frac{2}{3}} \quad (6)$$

where d_0 is mean initial radius of the fibre or particle, n is the number of elementary fibres in sample (800), l is a length of fibrous strand and ρ is the density of glass sample.

The time dependencies of normalised leach amount of glass components i ($i = Al, Si, B, Ca$) were obtained from concentrations of dissolved compound i (c_i) according to Eq. 7 (for static tests) or Eq. 8 (for SPFT tests)

$$NL_i = \frac{c_i}{x_i \frac{S_i}{V}} \quad (7)$$

$$NL_i^t = NL_i^{t-\Delta t} + \frac{c_i F \Delta t}{x_i S_i} \quad (8)$$

where NL_i is the normalised leach amount of compound i , t is time of interaction, Δt is the interval between sampling, x_i the weight ratio of i in glass, S the glass surface in contact with volume V of corrosion solution and F is the solution flow rate.

After the corrosion, an outer layer on fibres and par-

ticles was formed, previously made of SiO_2 (figure 1, figure 2). Assuming that the outer layer was formed by back precipitation (see lower), the surface of inner core was used for calculations.

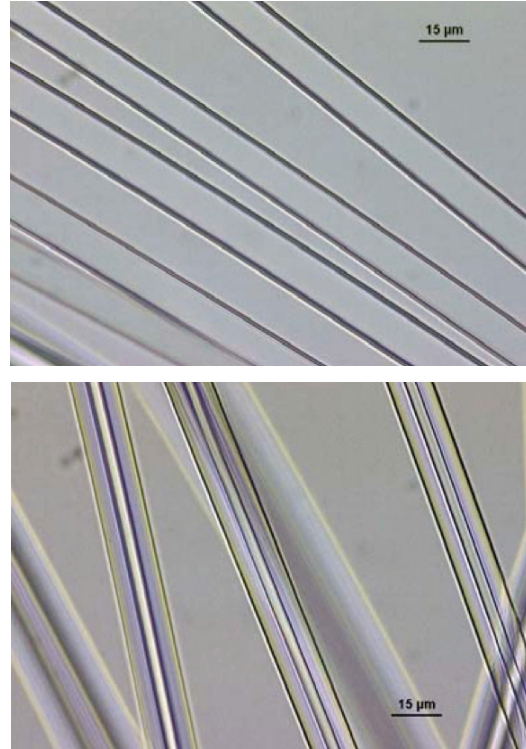


Fig. 1. Formation of outer layer on glass fibres. Static test in 2M HCl, 20°C, S/V = 1174 m⁻¹, after 6 hours (left) and 16 days of corrosion

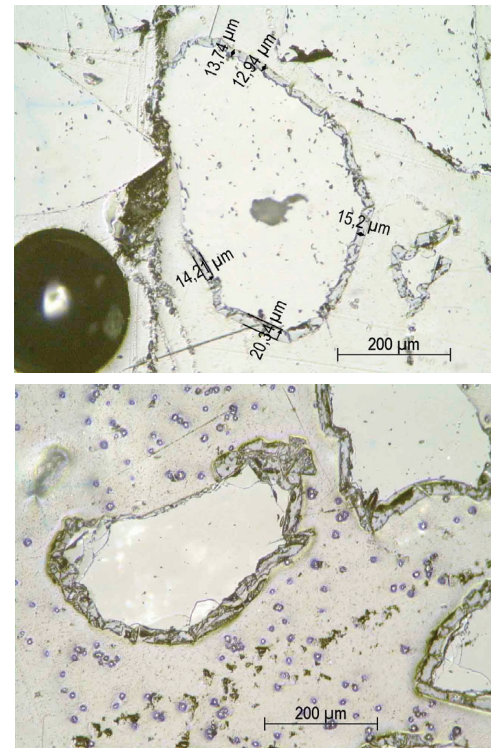


Fig. 2. Formation of outer layer on the particles of glass grain. Static test in 2M HCl, 20°C, S/V = 1174 m⁻¹, after 16 (left) and 32 days of corrosion

The typical time dependencies obtained from tests are shown in figures 3 and 4.

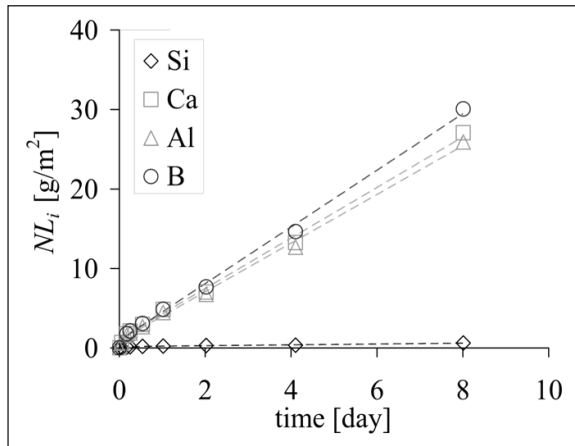


Fig. 3. The time dependence of NL_i . Static test in 2M HCl, $S/V = 1174 \text{ m}^{-1}$, 20°C , fibres

If the dissolution of glass is congruent, the time dependencies of NL_i should be the same. Similarly as in examples in figure 3 and figure 4, these time dependencies differ significantly, showing the incongruent dissolution. Typically, the NL_{Si} was much smaller than the NL_i for other components. This behaviour could be explained by back precipitation of Si in the form of silica and/or silicates. Another explanation could be by selective leaching of Ca, B and Al. As it was shown in our previous study [8], this possibility is not very plausible because the time dependencies of Ca, B and Al were often very similar and the probability of the same or similar diffusion coefficients of networking components Al, B and of Ca as typical network modifier is very low.

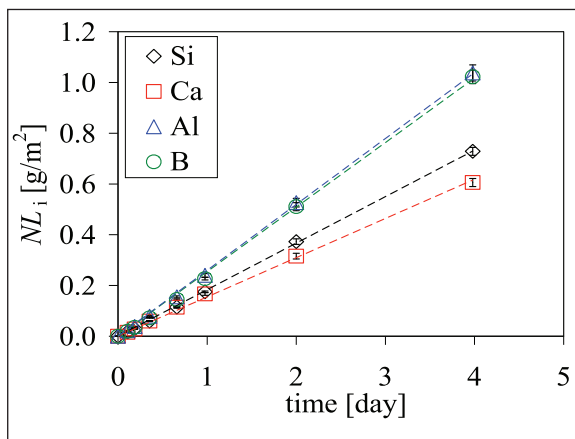


Fig. 4. The time dependence of NL_i . SPFT test in 0.2M NaOH, $F = 133 \text{ ml.d}^{-1}$, $F/S = 0.027 \mu\text{m.s}^{-1}$, 52°C , grains

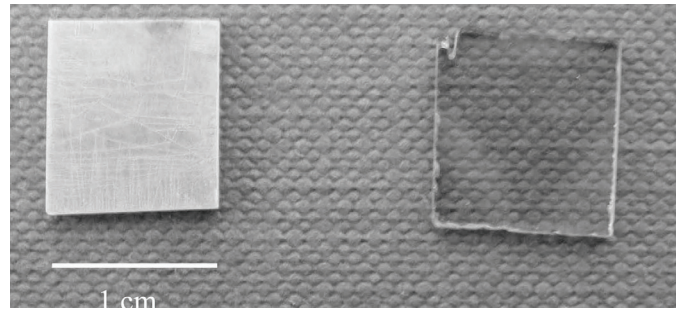


Fig. 5. Formation of secondary precipitated layer. Comparison of corroded (left) and uncorroded sample, SPFT test, samples dimensions $1 \times 1 \times 0.1 \text{ cm}$, 2M HCl, 51°C , $F = 130 \text{ ml.d}^{-1}$, $F/S = 2.16 \mu\text{m.s}^{-1}$

Moreover, the precipitated secondary layer was found on planar samples (figure 5) and as well as in form of practically pure SiO_2 outer layer on fibres (figures 1 and 2).

The dissolution rates were obtained by fitting the time dependencies of NL_i by Eq. 1 using the least squares method. The value $B + W$ and W from Eq. 1 then represent the initial and final dissolution rate [$\text{g.m}^{-2}\text{s}^{-1}$]. The movement of the solution — glass boundary in [m.s^{-1}] is given by Eqs. 9 and 10 for initial and final dissolution rate, respectively :

$$a_0 = \frac{B + W}{(1 - k^-)\rho} \quad (9)$$

$$a_n = \frac{W}{(1 - k^-)\rho} \quad (10)$$

The dissolution rates obtained for different test conditions are summarised in Table 3 for static tests and in Table 4 for SPFT tests. As the marker (A) for dissolution of E-glass, boron was used in most cases. Under several conditions, the total boron concentrations in the solutions were too low for analysis. In such a case, the Ca or Al was used.

The values of back precipitation ratio k^- for Si were calculated using Eqs. 11 and 12 both for initial and final stage of dissolution.

$$k_{t@0}^- = 1 - \frac{B_{\text{Si}} + W_{\text{Si}}}{B_{\text{A}} + W_{\text{A}}} \quad (11)$$

$$k_{t@\infty}^- = 1 - \frac{W_{\text{Si}}}{W_{\text{A}}} \quad (12)$$

It is obvious that these values are very high in most cases; especially in acid solution practically 90 % of Si precipitates back. This result could have interesting theoretical and practical consequences. If the back precipitation of Si occurs in the form of silica gel layer, the fibres or grains could be connected together. Then

sample type	T [°C]	S/V [m ⁻¹]	F [ml.d ⁻¹]	F/S [µm.s ⁻¹]	marker A	t [d]	Si a ₀ [µm.d ⁻¹]	Si a _n [µm.d ⁻¹]	A a ₀ [µm.d ⁻¹]	A a _n [µm.d ⁻¹]	k ⁻ (t→0)	k ⁻ (t→∞)	
fibres	20	12	0	0	Ca	1	0.45	0.45	5.29	2.23	0.92	0.80	
fibres					Ca	8	0.62	0.62	5.12	1.11	0.88	0.44	
fibres					117	Ca	1	0.35	0.29	4.49	2.21	0.92	0.87
fibres						Ca	8	0.41	0.04	4.36	1.01	0.91	0.96
fibres					1174	B	1	0.35	0.03	6.60	1.35	0.95	0.98
fibres						B	8	0.32	0.02	7.96	1.40	0.96	0.99
grains		12			B	1	0.28	0.05	0.78	0.36	0.64	0.87	
grains					B	8	0.23	0.08	0.76	0.38	0.70	0.78	
grains					B	32	0.27	0.08	0.78	0.36	0.66	0.76	
grains					1174	B	1	0.08	0.01	3.47	0.15	0.98	0.92
grains						B	8	0.08	0.005	3.39	0.13	0.98	0.96
grains						B	32	0.09	0.002	3.28	0.11	0.97	0.98
planar		12			B	1	0.06	0.06	1.47	0.56	0.96	0.89	
planar					B	8	0.17	0.17	1.51	0.54	0.89	0.68	
planar					B	32	0.12	0.12	1.39	0.43	0.92	0.73	

Table 3. Dissolution rates and back precipitation coefficients k⁻ evaluated from static tests under different conditions in 2M HCl.

sample type	T [°C]	S/V [m ⁻¹]	F [ml.d ⁻¹]	F/S [µm.s ⁻¹]	marker A	t [d]	Si a ₀ [µm.d ⁻¹]	Si a _n [µm.d ⁻¹]	A a ₀ [µm.d ⁻¹]	A a _n [µm.d ⁻¹]	k ⁻ (t→0)	k ⁻ (t→∞)
2M HCl												
fibres	20	3173	64	0.026	Al	1	0.11	0.11	1.45	1.45	0.93	0.93
fibres		7196	64	0.026	Al	1	0.11	0.11	1.39	1.39	0.92	0.92
fibres		6421	131	0.027	Ca	1	0.13	0.08	1.83	0.85	0.93	0.91
fibres		14844	129	0.026	Ca	1	0.11	0.07	1.59	0.90	0.93	0.93
fibres		12572	227	0.024	Ca	1	0.13	0.08	3.48	0.85	0.96	0.91
fibres		29831	250	0.027	Ca	1	0.11	0.05	2.53	0.68	0.96	0.92
fibres		544	58	0.308	Al	1	0.38	0.37	1.49	1.38	0.74	0.73
fibres		1106	117	0.308	Ca	1	0.27	0.27	1.97	1.25	0.86	0.79
fibres		2200	229	0.304	Ca	1	0.10	0.09	2.06	1.52	0.95	0.94
fibres		51	14928	134	0.027	B	1	0.24	0.24	10.5	2.62	0.98
fibres	B					2	0.30	0.30	10.4	2.98	0.97	0.90
fibres	85	14977	133	0.027	B	1	0.24	0.24	15.2	1.54	0.98	0.80
fibres					B	2	0.30	0.30	15.2	0.62	0.98	0.46
grains	51	21510	133	0.027	B	1	0.23	0.23	5.82	5.82	0.96	0.96
grains					B	2	0.22	0.22	5.43	5.43	0.96	0.96
planar		207	130	2.3	B	1	2.46	2.46	19.6	13.8	0.87	0.82
planar					B	2	3.20	3.20	19.8	9.92	0.84	0.68
planar					B	4	3.72	3.72	19.8	8.42	0.81	0.56
0.2M NaOH												
fibres	52	15053	133	0.027	B	4	0.12	0.07	0.28	0.15	0.57	0.57
grains		21505	132	0.027	B	4	0.10	0.10	0.07	0.07	0.28	0.28

Table 4. Dissolution rates and back precipitation coefficients k⁻ evaluated from SPFT tests under different conditions in 2M HCl and 0.2M NaOH.

